Temporal variations of non-volcanic tremor (NVT) locations in the Mexican subduction zone: Finding the NVT sweet spot.

Allen Husker, Vladimir Kostoglodov, Victor Cruz-Atienza, Denis Legrand,
N.M. Shapiro, Juan S. Payero, Michel Campillo, Eduardo Huesca-Pérez

HAL Id: hal-00706692
https://hal.archives-ouvertes.fr/hal-00706692

Submitted on 11 Jun 2012

Temporal variations of non-volcanic tremor (NVT) locations in the Mexican subduction zone: finding the NVT sweet spot

Allen L. Husker[1*]; Vladimir Kostoglodov[1]; Victor M. Cruz-Atienza[1]; Denis Legrand[1]; Nikolai M. Shapiro[2]; Juan S. Payero[1]; Michel Campillo[3]; Eduardo Huesca-Pérez[1]

[1]*Instituto de Geofísica, Universidad Nacional Autónoma de México, Av. Ciudad Universitaria 3000, Col. Copilco, Del. Coyoacan, 04360 México, DF, México*

[2]*Institut de Physique du Globe de Paris, Sorbonne Paris Cité, UMR7154 CNRS, 75238 Paris, Cedex 05, France*

[3]*LGIT, CNRS, Observatoire de Grenoble, Université Joseph Fourier, Maison des Géosciences BP 53 38041 Grenoble Cedex 9, France.*

allen@geofisica.unam.mx

Instituto de Geofísica, Universidad Nacional Autónoma de México, Av. Ciudad Universitaria 3000, Col. Copilco, Del. Coyoacan, 04360 México, DF, México

Abstract

Epicentral locations of non-volcanic tremors (NVT) in the Mexican subduction zone are determined from the peak of the energy spatial distribution and examined over time. NVT is found to occur persistently at a distance of ~215 km from the trench, which we term the "Sweet Spot" because this region probably has the proper conditions (i.e. temperature, pressure, and fluid content) for the NVT to occur with minimum shear slip. High-energy NVT episodes are also observed every few months, extending ~190 km to ~220 km from

the trench with durations of a few weeks. During the 2006 slow slip event (SSE) the duration and the recurrence rate of the NVT episodes increased. Low-energy episodes were also observed, independent from the high-energy episodes, ~150 km to ~190 km from the trench during the 2006 SSE. Both the high and low energy episodes were made up of many individual NVT's that had a range of energy-release-rates. However, the highest energy-release-rates of the high-energy episodes were consistently double those of the low-energy episodes and the persistent activity at the Sweet Spot. We suggest that all of the high-energy episodes are evidence of small, short repeat interval SSE. Given this model, the increased recurrence rate of the high-energy NVT episodes during the 2006 long term SSE implies that short term SSE's also increase during the SSE and are therefore triggered by the SSE.

1. Introduction

Non-volcanic tremor (NVT) in the Japan, Cascadia, and Costa Rican subduction zones typically occurs when the slab is at the depth of 30 - 50 km [*e.g. Obara* 2002; *Brown et al.,* 2009; *Ghosh et al.,* 2009; *Kao et al.,* 2009]. Recent precise detections of Low Frequency Earthquakes (LFE), which make up NVT, locate the LFE's on the interface between the subducting oceanic plate and overriding mantle wedge [*Brown et al.*, 2009; *Kato et al.*, 2010]. In Guerrero, Mexico, the slab descends from the Middle American Trench to ~40 km depth at about 150 km from the trench. It then remains horizontal near 40 km depth for ~140 km [*Pérez-Campos et al.,* 2008; *Kim et al.,* 2010] (Figure 1). At ~290 km from the trench the slab plunges deeper into the mantle [*Pérez-Campos et al.,* 2008; *Husker and Davis*, 2009; *Kim et al.,* 2010]. NVT in Mexico occur in a 75 km long zone above the 140 km horizontal slab, far from the mantle wedge (Figure 1) [Payero et al., 2008]. As a result of the slab geometry, the commonly used terms 'updip' and 'downdip'

can be misleading in the sub-horizontal section of the slab where there is no dip, but we use the terms for clarity when describing location along the slab.

SSE has been observed in two types: (1) short-term (small repeat interval), small magnitude SSE and (2) long-term (long repeat interval), large magnitude SSE [e.g. *Hirose and Obara*, 2005; *Obara and Hirose*, 2006; *Obara*, 2010; *Obara*, 2011]. The short-term SSE and NVT occur simultaneously in space and time. On the other hand, the long-term SSE occurs updip from the source region of NVT and short-term SSE. The episodic tremor and slip (ETS) observed in Cascadia is then the short-term SSE, while the 2006 Mexican SSE observed to be updip from the NVT belongs to the long-term SSE [*Rogers and Dragert*, 2003; *Kostoglodov et al.*, 2010; *Obara*, 2011].

Previous studies have linked evidence of high pore fluid pressure to subduction zones where NVT occurs [e.g. *Obara*, 2002; *Shelly et al.*, 2006; *Audet et al.*, 2009]. In Mexico, studies have presented a number of possible sources of fluid in the crust above the flat slab. These include the release of trapped water from the slab after passing over-pressurized impermeable boundaries [*Song et al.*, 2009; *Kim et al.*, 2010], water releasing metamorphic phase changes [*Manea et al.*, 2004; *Manea et al.* 2010], and water squeezed from the slab due to slab bending [*Jödicke et al.* 2006]. Evidence from a magnetotelluric study [*Jödicke et al.* 2006] and a seismic velocity tomography [*Huesca-Pérez and Husker*, submitted] suggests that water is present throughout the entire lower crust above the flat slab and that the amount of fluid increases in the downdip direction. The evidence from the magnetotelluric study and tomography do not distinguish which of the fluid sources is most probable and it may be a combination of the three.

The seismic network that measured the NVT in Mexico during the 2006 SSE was a very dense (~6 km spacing) temporary line of broadband seismometers installed

perpendicular to the trench from 2005 - 2007 called the MesoAmerican Subduction Experiment (MASE) [*http://www.tectonics.caltech.edu/mase/*] (Figure 1). The original NVT study [*Payero et al.*, 2008] of data from MASE used cross-correlations of envelopes of NVT [*Obara*, 2002] in order to locate the tremor. The method suffers from imprecise locations because correlating emergent windows over many minutes or hours causes inexact, rolling cross-correlation peaks. In addition, the locations were limited because the MASE station arrangement was approximately a one-dimensional line. In order to bypass these limitations, *Kostoglodov et al.* [2010] plotted the NVT energy (square of velocity) of the north component recorded at each station during the two and a half year duration of MASE to map the region of NVT along the MASE line.

In this study, we determine epicenters of all the individual NVT's during that period using an energy location method. We then analyze the epicentral locations of individual NVT's over time. When there are a large number of individual NVT's over an interval of a few days, this is considered an episode of NVT as defined by other authors [*e.g. Audet et al.*, 2009; *Obara*, 2010]. *Kostoglodov et al.* [2010] exclusively analyzed episodes of activity, although they were described as bursts since the individual NVT's that make up an episode were not seen in that study. We then analyze the energy of the NVT in different regions and its association with long term and short term SSE's in Mexico.

2. NVT Location Method

The location technique employed in this study is similar to amplitude location methods in volcano studies [e.g. *Legrand et al.*, 2000; *Battaglia and Aki*, 2003; *Taisne et al.*, 2011]. The difference between the amplitude location method with volcanic tremor and with NVT is that volcanic tremor is largely isotropic with P waves dominating while NVT

appears to have a double couple source with S waves dominating [*Obara et al.*, 2002; *Shelly et al.*, 2007]. In our data, the energy of the north component is systematically greater than the east component, which is greater than the vertical component with the location of the energy maximums and the energy falloff corresponding between all components (Figure 2). It is very difficult to generate radiation patterns with corresponding shapes between all components from an ideal single double couple source, as maximums in the radiation pattern for S waves are nodes for P waves and vice versa. There is evidence that NVT is made up of many small low frequency earthquakes (LFE's) [*Shelly et al.*, 2007]. Multiple small horizontal approximately east-west striking double-couple sources with rakes pointing northward generated over a small area could create the observed energy pattern. This NVT mechanism model is supported by the general north-south Cocos slab and North American plate convergence in this region [*DeMets et al.*, 1994]. Scattering plays a role in diminishing the observed radiation pattern as well, but it obviously has not completely eliminated the radiation pattern because the energy level is different in each of the three components. Assuming this dislocation model for the observed data, the energy maximum at the surface is the location of the epicenter. There may be small deviations based on small differences in the focal mechanism, particularly the dip, but this effect must be small or the observed energy shapes would substantially differ between components.

Onsets and durations of NVT were automatically determined using the energy of median filtered envelopes of seismograms [*Husker et al.*, 2010]. An individual NVT was established when the energy averaged across all stations surpassed an empirically determined threshold. The energy was then summed into two-week intervals and presented over time (2005 – 2007 the duration of MASE) [*Kostoglodov et al.*, 2010]. The background of Figure 3 was created in the same way. This gave the broad details of NVT location along

the MASE profile during this period and showed a significant increase of NVT during the 2006 SSE [*Payero et al.*, 2008; *Kostoglodov et al.*, 2010; *Vergnolle et al.,* 2010]. However, the summing of NVT energy in previous studies only showed the dominant NVT trend and not the complete spatio-temporal variations of smaller individual NVT's.

In order to determine the temporal and spatial variations of the NVT, each tremor was located using the energy falloff from the source with distance due to geometrical spreading and intrinsic attenuation (Equation 1). The goal of the inversion technique to locate the NVTs was to find the epicenter of each event along the MASE array. The one-dimensional shape of the seismological network does not allow for solving for a focal mechanism, the area, or the depth of the NVT, as there are too many degrees of freedom that trade-off with one another. We only determine the epicenters using the following simple equation:

$$E = \frac{C}{r^2} e^{\frac{r\omega}{vQ}},$$ **(1)**

where E is the energy (summed squared velocity) of the NVT measured at each station, C is a constant which is related to the energy at the source, r is the distance between source and receiver, ω is the peak frequency, v is the average seismic velocity of the medium, and Q is the quality factor. The latitude and longitude of the epicenter and C were the parameters solved to minimize the least-square error between the observed and theoretical energy profiles along the array [e.g. *Aster et al.*, 2005]. Only the energy, E, from the northern component was used in the inversion as it had the greatest signal to noise ratio. Site effects were removed before inverting for the location using coda-determined site factors [*Husker et al.*, 2010]. ω was set to be 1.5 Hz (x 2π) since the seismograms were filtered 1 – 2 Hz due to the range of detectable NVT frequencies (~1 – 10 Hz) and ambient noise (> 2 Hz).

NVT's have a more or less fixed spectrum, unlike earthquakes, so a small frequency band is representative of the overall energy [*Aguiar et al.*, 2009; *Kostoglodov et al.*, 2010]. The quality factor Q was set to 276 determined for this frequency range from attenuation studies in Mexico [*Garcia et al.*, 2004]. The depth was conditionally set to 40 km as many recent studies have found all or most NVT at or just above the plate interface [*Shelly et al.*, 2007; *Brown et al.*, 2009]. However these studies use limited time windows that may create limitations of allowed moveouts forcing only detections of deeper sources. *Kao et al.* [2009] found sources throughout the crust in Cascadia with concentrations of NVT 10 - 20 km above the plate interface. Therefore, a range of depths was implemented in our inversion, but the results changed very little because it is just a search for the maximum of the energy parabola as already mentioned. Initial values for latitude, longitude, and C were chosen from the station that recorded the maximum energy. Location results with standard deviations greater than 1% of the final value of the latitude or the longitude were thrown out. Figure 4 depicts two examples of the inversion results.

3. NVT Locations over time

The NVT epicenter location results are shown in Figure 1 and largely agree with previous location studies [*Payero et al.*, 2008; *Kostoglodov et al.*, 2010]. Figure 3 and the NVT.mp4 animation in the auxiliary material show how the NVT epicenter locations change over time. Figure 3 depicts almost continuously occurring NVT near 215 km from the trench, which we label the Sweet Spot. The term "Sweet Spot" is most commonly used in baseball and acoustics to refer to a limited zone with the correct conditions to create a particular effect (e.g. http://en.wikipedia.org/wiki/Sweet_spot), and it is used here with the same understanding. There is inter-episode NVT on the downdip side of the NVT activity

in Cascadia as well, but it is not always in the same location along strike of the trench [*Wech and Creager*, 2008]. In southwest Japan, the studies there focus on NVT concentrations along strike, rather than perpendicular to the trench [e.g. *Obara et al.*, 2011]. There are Sweet Spots observed there as well where certain points along strike exhibit continuous inter-episode NVT, but it is not clear if they are on the downdip side of the NVT zone as in Cascadia and Mexico [*Obara et al.*, 2010].

In addition to the continuous NVT activity at the Sweet Spot, there are NVT episodes occurring every few months. The episodes, which last a few days to weeks, are composed of many NVT's. The background of Figure 3 is the sum of all the individual NVT's over two week intervals. Thus, higher sums (E > 40 X 10^{-12} m^2/s; red background) can be due to more individual NVT's and/or higher energy tremors. The coincidence of large numbers of NVT's and the high summed energy (red background) are considered high-energy episodes. It is difficult to determine if there is periodicity of the episodes as only 3 intervals between episodes occur outside of the 2006 SSE. Throughout the 2006 SSE, the frequency and duration of the NVT episodes increased. During the episodes, NVT epicenters extend updip from the Sweet Spot, near 215 km from the trench (Figure 3). The NVT epicenters in the episodes are observed to migrate or progress updip at a rate of ~1 - 20 km / day similar to migration observed in Cascadia [*Wech and Creager*, 2011]. During the 2006 SSE it was not possible to observe migration due to much higher activity throughout the NVT region.

Lower energy NVT epicenters were also detected further updip with their own separate NVT episodes. Figure 3 depicts clusters of many NVT's during the 2006 SSE that are updip from the high-energy episodes. Their summed NVT energy is much lower than the downdip epicenters, and therefore they were not observed by *Kostoglodov et al.* [2010]

and do not appear as episodes in Figure 3. In order to observe the summed energy of the updip tremors exclusively, only the energy profiles from NVT epicenters < 190 km from the trench are summed in the background of Figure 5. The updip, low energy NVT epicenters (green dots, Figure 5), which have total energy about four times lower than the dowdip NVTs, start to occur about 1 month after the beginning of the SSE, and the strongest updip NVT's do not occur until at least 3 months after the initiation of the SSE.

NVT durations have been found to vary from seconds to days, but the amplitude of tremor remains nearly constant [e.g. *Aguiar et al.*, 2009]. Thus, the energy of NVT is nearly linearly correlated with the duration of the individual NVT. Although we find that the energy (*C*) and the duration (Δt) are correlated (Figure 6a), NVT in the high-energy zone (> 190 km from the trench) also exhibits greater amplitudes than the NVT in the low energy zone (< 190 km from the trench) (Figure 6b). The duration-normalized energy (*C*/Δt, also called the energy release rate) of NVT in Figure 6 would be roughly constant over time if *C* were always proportional to Δt. Instead, the updip NVT's are limited to ~0.4 of the largest downdip NVT's (Figure 6b) implying limited amplitudes as well. In addition, apart from a few events in June-July 2005 (which may acutally be a small episode) the NVT activity between episodes during the whole time span is upper-bounded by the ~0.4 level below which the updip, low-energy NVTs are confined (Figure 6b). This shows that during the episodes within the high-energy zone, the NVT energy release rate increases, contrary to what has been observed in Cascadia, where the average rate does not fluctuate [*Aguiar et al.*, 2009]. *Wech and Creager* [2011] also found that there is greater NVT energy downdip in Cascadia, but this is purely due to duration of the NVT episodes and the quantity of NVT's in those episodes.

The majority of the 2006 SSE dislocation extended to approximately 165 km from

the trench [*Larson et al.*, 2007; *Kostoglodov et al.*, 2010; *Vergnolle et al.*, 2010]. A more recent inversion found small amounts of slip as far as 215 km from the trench, but the maximum was always updip from the NVT Sweet Spot [*Radiguet et al.*, 2010] (Figure 7). NVT did not occur within the peak of the slipping front of the SSE and primarily only overlapped the downdip edge of it (Figure 7) [*Larson et al.*, 2007; *Radiguet et al.*, 2010; *Kostoglodov et al.*, 2010; *Vergnolle et al.*, 2010]. This confirms, along the whole NVT region, the spatio-temporal separation between NVT and SSE previously observation by *Kostoglodov et al.* [2010] over the NVT high-energy segment. However, the updip, low energy NVT occurs concurrently with the 2006 SSE and appears to be a direct effect of the SSE although the low energy NVT is also limited spatially (> 150 km from the trench). The updip limit of the NVT is very close to the corner of the slab (Figures 1, 7).

4. Discussion

4.1 NVT episodes provide evidence for short term SSE

The observation of spatially separated SSE and NVT may occur because there are two types of slow slip events as seen in the southwest Japan subduction zone [*Obara*, 2010; *Obara*, 2011]. There are short-term (small repeat interval), small magnitude SSE that occur downdip from the long-term (long repeat interval), large magnitude SSE [*Hirose and Obara*, 2005; *Obara*, 2010; *Obara*, 2011]. In the case of Japan, both types of SSE are accompanied by NVT, however more NVT occur during the short term SSE. Thus, *Obara* [2011] categorized the Cascadia episodic tremor and slip (ETS) as short term SSE. Due to the previously observed separation of NVT's from the SSE's in Mexico [*Kostoglodov et al.*, 2010], those SSE's were classified as long term SSE's [*Obara*, 2011].

Varios studies have suggested that with the absence of detailed geodetic

measurements, NVT episodes could be used to identify short term SSE [*Aguiar et al.*, 2009; *Wech and Creager*, 2008; *Obara* 2011]. The observation of NVT episodes downdip from the long term SSE zone in Mexico provides evidence for short term SSE. In addition, possible short term SSE's have been detected within the NVT region [*Vergnolle et al.*, 2010]. Detections were so small within the GPS signal that it was impossible to determine the precise location, but the strongest signals were all located well within the NVT region [*Vergnolle et al.*, 2010]. With each detectable short term SSE a high energy NVT episode occurred [*Kostoglodov et al.*, 2010; *Vergnolle et al.*, 2010]. High-energy NVT episodes with no clear short term SSE were also observed, but short term SSE detection is problematic because the corresponding displacements recorded by GPS are almost at the noise level of the position time series [*Vergnolle et al.*, 2010]. Thus, the model seen in Japan of cyclical short term SSE's with strong NVT episodes and long term SSE's with weak NVT episodes follows the evidence seen in Mexico [*Obara*, 2011]. The increased rate of the NVT episodes during the 2006 long term SSE suggests that the short term SSE's are triggered by the long term SSE.

4.2 Conditions for NVT

The long term SSE region in Mexico aligns with an ultra slow velocity layer (USL) found between the slab and overriding plate that is probably a remnant mantle wedge from before the slab was horizontal [*Pérez-Campos et al.*, 2008; *Song et al.*, 2009]. The high energy NVT region, which is now considered due to a short term SSE, aligns with a moderate USL [*Song et al.*, 2009]. The USL's are evidence of high pore fluid pressure that allows the two types of SSE's to occur. These observations coincide with those by *Kato et al.* [2010] where the long term SSE's occur in a highly pressurized region, while short term

SSE's and their associated NVT's occur in a modestly pressurized region. NVT's in Mexico do occur directly because of the long term SSE, but they do not extend throughout the entire long term SSE region (Figures 1, 3, 5, 7), and there is no evidence in Mexico of how the short term SSE region aligns with the down dip NVT. Thus, the limited NVT zone within the long term SSE is evidence that NVT might require modestly high pore fluid pressure.

This may suggest that the Sweet Spot is the zone with the proper pressure and/or temperature for NVT to persistently occur and that NVT that occur outside of the Sweet Spot may require an additional input. Evidence of a pressure change was observed during the 2006 SSE when the average seismic velocity within NVT region in the crust was observed to decrease, indicating increased dilation [*Rivet et al.*, 2011]. As mentioned, during the 2006 SSE, NVT was observed farther from the Sweet Spot than at any other time during this study coinciding with the observed dilation increase.

5. Conclusions

This study found that persistent background NVT occurs approximately 215 km from the trench in a flat section of the slab in Guerrero, Mexico. High-energy NVT tremor episodes occur every few months with durations of a few weeks. The recurrence rate of those episodes increased during the 2006 SSE. During that same SSE, low energy NVT were observed closer to the trench than at any other time, between 150 and 190 km from the trench. This NVT activity was about four times less energetic than further down-dip and had a lower energy-release-rate. The high-energy NVT zone, between 190 to 220 km from the trench, coincides with a region of modestly high pore fluid pressure in between the slab and overriding plate. The spot 215 km from the trench has the necessary conditions to

generate NVT persistently and so we refer to it as the NVT Sweet Spot. All NVT generated out of the Sweet Spot require an additional input to generate NVT. We suggest that the additional stress and increased dilation for fluid content necessary to generate NVT outside of the Sweet Spot are the SSE's. Assuming that each high-energy NVT episode therefore indicates a short term SSE, the increase in the number of NVT episodes during the long term SSE suggests that short term SSE's can be triggered by SSE's. These observations and interpretation of long and short term SSE coincide with observations in Japan where SSE's are found to occur closer to the trench than short term SSE's, the two interact, and NVT's coincide with short term SSE's [*Hirose and Obara*, 2005; *Obara*, 2010; *Obara*, 2011].

References

Aguiar, A. C., T. I. Melbourne, and C. W. Scrivner (2009), Moment release rate of Cascadia tremor constrained by GPS, *J. Geophys. Res.*, *114*, B00A05, doi:10.1029/2008JB005909.

Aster, R. C., B. Borchers, and C. H. Thurber (2005), *Parameter Estimation and Inverse Problems*, Elsevier, San Diego, USA.

Audet, P., M. G. Bostock, N. I. Christensen, and S. M. Peacock (2009), Seismic evidence for overpressured subducted oceanic crust and megathrust fault sealing, *Nature, 457*, 76–78, doi:10/1038/nature07650.

Battaglia, J., and K. Aki (2003), Location of seismic events and eruptive fissures on the Piton de la Fournaise volcano using seismic amplitudes, *J. Geophy. Res., 108*, 2364, 10.1029/2002jb002193.

Brown, J. R., G. C. Beroza, S. Ide, K. Ohta, D. R. Shelly, S. Y. Schwartz, W. Rabbel, M. Thorwart, and H. Kao (2009), Deep low-frequency earthquakes in tremor localize to the plate interface in multiple subduction zones, *Geophys. Res. Lett., 36*, L19306, doi:10.1029/2009GL040027.

DeMets, C., R. G. Gordon, D. F. Argus, S. Stein (1994), Effect of recent revisions to the geomagnetic reversal time scale on estimates of current plate motions. *Geophys. Res. Lett. 21*(20), 2191-2194.

Garcia, D., S. K. Singh, M. Herraiz, J. F. Pacheco, and M. Ordaz (2004), Inslab Earthquakes of Central Mexico: Q, Source Spectra, and Stress Drop, *Bull. Seismol. Soc. Am., 94*(3), 789-802.

Ghosh, A., J. E. Vidale, J. R. Sweet, K. C. Creager, and A. G. Wech (2009), Tremor patches at Cascadia revealed by array analysis, *Geophys. Res. Lett., 36*, L17316, doi:10.1029/2009GL039080.

Hirose, H., and K. Obara (2005), Repeating short- and long-term slow slip events with deep tremor activity around the Bungo channel region, southwest Japan, *Earth Planets Space, 57*, 961-972.

Husker, A., S. Peyrat, N. Shapiro, and V. Kostoglodov (2010), Automatic non-volcanic tremor detection in the Mexican subduction zone, *Geofis. Int.*, *49*(1), 17-25.

Jödicke, H., A. Jording, L. Ferrari, J. Arzate, K. Mezger, and L. Rüpke (2006), Fluid release from the subducted Cocos plate and partial melting of the crust deduced from magnetotelluric studies in southern Mexico: Implications for the generation of volcanism and subduction dynamics, *J. Geophys. Res.*, *111*, B08102, doi:10.1029/2005JB003739.

Kao, H., S.-J. Shan, H. Dragert, and G. Rogers (2009), Northern Cascadia episodic tremor and slip: A decade of tremor observations from 1997 to 2007, *J. Geophys. Res.*, *114*, B00A12, doi:10.1029/2008JB006046.

Kato, A., T. Iidaka, R. Ikuta, Y. Yoshida, K. Katsumata, T. Iwasaki, S. Sakai, C. Thurber, N. Tsumura, K. Yamaoka, T. Watanabe, T. Kunitomo, F. Yamazaki, M. Okubo, S. Suzuki, N. Hirata (2010), Variations of fluid pressure within the subducting oceanic crust and slow earthquakes, *Geophys. Res. Lett.*, *37*, L14310, doi:10.1029/2010GL043723.

Kim, Y., R. W. Clayton, and J. M. Jackson (2010), Geometry and seismic properties of the subducting Cocos plate in central Mexico, *J. Geophys. Res.*, *115*(B6), B06310.

Kostoglodov, V., A. Husker, N. M. Shapiro, J. S. Payero, M. Campillo, N. Cotte, R. Clayton (2010), 2006 Slow Slip Event and Nonvolcanic Tremor in the Mexican Subduction Zone, *Geophys. Res. Lett.*, *37*, L24301, doi:10.1029/2010GL045424.

Larson, K. M., V. Kostoglodov, S. Miyazaki, and J. A. S. Santiago (2007), The 2006 aseismic slow slip event in Guerrero, Mexico: New results from GPS, *Geophys. Res. Lett.*, *34*(13), 1-5.

Legrand, D., S. Kaneshima, H. Kawakatsu (2000), Moment tensor analysis of near-

field broadband waveforms observed at Aso Volcano, Japan, *J. Vol. Geotherm. Res.*, *101*, 155-169.

Manea, V. C., and M. Manea (2010), Flat-Slab Thermal Structure and Evolution Beneath Central Mexico, *Pure and App. Geophys.*, doi: 10.1007/s00024-010-0207-9.

Manea, V. C., M. Manea, V. Kostoglodov, C. A. Currie, and G. Sewell (2004), Thermal structure, coupling and metamorphism in the Mexican subduction zone beneath Guerrero, *Geophys J Int*, *158*(2), 775-784.

Obara, K. (2002), Nonvolcanic Deep Tremor Associated with Subduction in Southwest Japan, *Science*, *296*(5573), 1679-1681.

Obara, K. (2010), Phenomenology of deep slow earthquake family in southwest Japan: Spatiotemporal characteristics and segmentation, *J. Geophys. Res.-Solid Earth*, *115*, B00A25-doi:10.1029/2008JB006048.

Obara, K. (2011), Characteristics and interactions between non-volcanic tremor and related slow earthquakes in the Nankai subduction zone, southwest Japan, *J. Geodynamics*, *52*, 229-248.

Obara, K. and H.Hirose (2006), Non-volcanic deep low-frequency tremors accompanying slow slips in the southwest Japan subduction zone, *Tectonophys.*, *417*, 33-51.

Payero, J. S., V. Kostoglodov, N. Shapiro, T. Mikumo, A. Iglesias, X. Pérez-Campos, and R. W. Clayton (2008), Nonvolcanic tremor observed in the Mexican subduction zone, *Geophys. Res. Lett.*, *35*(7).

Pérez-Campos, X., Y. Kim, A. Husker, P. M. Davis, R. W. Clayton, A. Iglesias, J. F. Pacheco, S. K. Singh, V. C. Manea, and M. Gurnis (2008), Horizontal subduction and truncation of the Cocos Plate beneath central Mexico, *Geophys. Res. Lett.*, *35*.

Radiguet M., F. Cotton, M. Vergnolle, M. Campillo, B. Valette, V. Kostoglodov, and N. Cotte (2010), Spatial and temporal evolution of a long term slow slip event, the 2006 Guerrero Slow Slip Event, *Geophys. J. Int.*, doi: 10.1111/j.1365-246X.2010.04866.x.

Rivet, D., M. Campillo, N. M. Shapiro, V. Cruz-Atienza, M. Radiguet, N. Cotte, V. Kostoglodov (2011), Seismic evidence of nonlinear crustal deformation during a large slow slip event in Mexico, *Geophys. Res. Lett. 38*(8), L08308.

Rogers, F., and H. Dragert (2003), Episodic Tremor and Slip on the Cascadia Subduction Zone: The Chatter of Silent Slip, *Science*, *300*, 1942-1943 doi: 10.1126/science.1084783.

Schwartz, S. Y. and J. M. Rokosky (2007), Slow slip events and seismic tremor at circum-Pacific subduction zones. *Rev. Geophys.* 45.

Shelly, D. R., G. C. Beroza, and S. Ide (2007), Non-volcanic tremor and low-frequency earthquake swarms, *Nature*, *446*(7133), 305-307.

Shelly, D. R., G. C. Beroza, S. Ide, and S. Nakamula (2006), Low-frequency earthquakes in Shikoku, Japan, and their relationship to episodic tremor and slip, *Nature*, *442*(7099), 188-191.

Song, T. A., D. V. Helmberger, M. R. Brudzinski, R. W. Clayton, P. Davis, X. Perez-Campos, S. K. Singh (2009), Subducting Slab Ultra-Slow Velocity Layer Coincident with Silent Earthquakes in Southern Mexico, *Science*, *324*(5926), 502-506.

Taisne, B., F. Brenguier, N. M. Shapiro, and V. Ferrazzin, Imaging the dynamics of magma propagation using radiated seismic intensity, *Geophys. Res. Lett.*, 38, L04304, doi:10.1029/2010GL046068, 2011.

Vergnolle, M., A. Walpersdorf, V. Kostoglodov, P. Tregoning, J. A. Santiago, N. Cotte, S. I. Franco (2010), Slow slip events in Mexico revised from the processing of 11 year

GPS observations, *J. Geophys. Res.*, *115*(B8), B08403.

Wech, A. G., and K. C. Creager (2008), Automated detection and location of Cascadia

tremor, *Geophys. Res. Lett.*, *35*, L20302, doi:10.1029/2008GL035458.

Wech, A. and K. C. Creager (2011), A continuum of stress, strength and slip in the Cascadia

subduction zone, *Nature Geoscience*, *4*, 624-628, doi:10.1038/ngeo1215.

Figure Captions

Figure 1. Map of the NVT epicenters (dots) found in this study. The orange dots are the downdip epicenters. The gray dots are the inter-episode epicenters. The green dots are the updip epicenters. Inset: setting of the study area, red rectangle. Main figure: The black triangles are the locations of the MASE seismometers. The profile A-A' is the same profile shown in Figures 3 - 5. The shape of the slab (purple) and the location of the 2006 SSE (yellow) are shown in the horizontal cartoon in the figure for clarity, but the cartoon should actually be vertical, extending into the Earth from the MASE array. The distance markers are measured from the Middle American Trench (MAT). The dashed line, MAT, is the Middle America Trench. Shaded regions along the coast are the rupture areas of the most resent large subduction thrust earthquakes annotated with its year of occurrence. Blue arrow indicate the convergence velocity vector according to the NUVEl 1 A model [*DeMets et al.*, 1994].

Figure 2. Example tremor seismogram. This is from an NVT episode recorded at the station TONA approximately 200 km from the trench [Perez-Campos et al., 2008]. The northern component is clearly larger than the eastern component. The vertical component is clearly the smallest component. This was typical for the tremor measured in this study.

Figure 3. The NVT energy and epicenter locations. In the top panel the background color is the NVT seismic energy measured at the surface summed in two-week intervals as described by *Kostoglodov et al.* [2010]. This figure differs slightly from Figure 2B of *Kostoglodov et al.* [2010] because energy profiles that did not meet the error criteria described in the localization method were considered spurious, non-NVT events and not

used in the sum. The dots are the epicenters of the NVT from the inversion. The dots sometimes do not align exactly with the background energy profile due to how the summed energy is binned into 15-day intervals. The green dots are the trenchward, updip, low-energy epicenters. The orange dots are the downdip epicenters with mostly high energies as noted by the background colors. The gray dots are the inter-episode epicenters. The y-axis is the time and the x-axis is distance from the trench. The cross-section of the continental crust and slab in the lower panel (profile A - A' from Figure 1) aligns with the upper panel in order to demonstrate the details from the electrical conductivity measured in the crust [*Jödicke et al.*, 2006]. The blue color in the cross-section represents high resistivity and low conductivity, and red is the opposite. Temperature contours in degrees Celsius from *Manea et al.* [2004] are also shown in the cross-section.

Figure 4. Example results from the inversion. Energy in the figure was normalized to the maximum measured energy of each respective NVT episode. The red energy profile is from an updip NVT epicenter (183.6 km ± 4.4 km) that occurred May 21, 2006 and the blue is from an inter-episode NVT epicenter that occurred December 25, 2005 (215.5 km ± 13.7 km). The points are the data and the lines are the synthetic energy profiles generated from Equation 1 after the locations have been determined. The synthetic lines are both above 1 since the figure is normalized to the measured energy peaks and there is probably an error in the location due to distance from the MASE profile and the fixed depth. The blue inter-episode NVT data was particularly noisy due to it being low amplitude. Stations near the coast (~70 km from the trench) often had elevated energies due to noise bias from weather storms as seen in these two events. Although noisy storm data from the coastal stations was included in the inversion, the effect to the epicentral locations was quite small (≤ 1 km).

When the coastal stations were removed from the inversion the locations were 182.7 km ± 3.2 km and 214.9 km ± 12.2 km respectively.
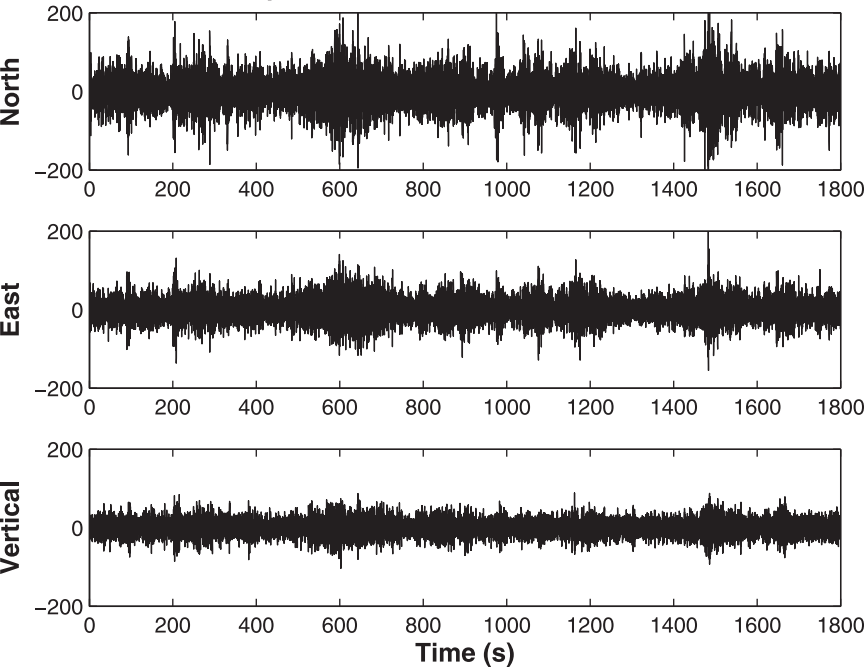
Figure 5. The seismic energy (background colors) measured at the surface from only the low-energy, updip NVT from Figure 3. The high-energy, downdip NVT (orange dots) were not used to generate the seismic energy image in order to observe the low-energy episodes, which are a factor of ~4 less energetic. The highest energy in this figure is about 13 X 10^{-12} m^2/s, which is too small to be observed clearly in Figure 3. The gray dots are the inter-episode NVT's.
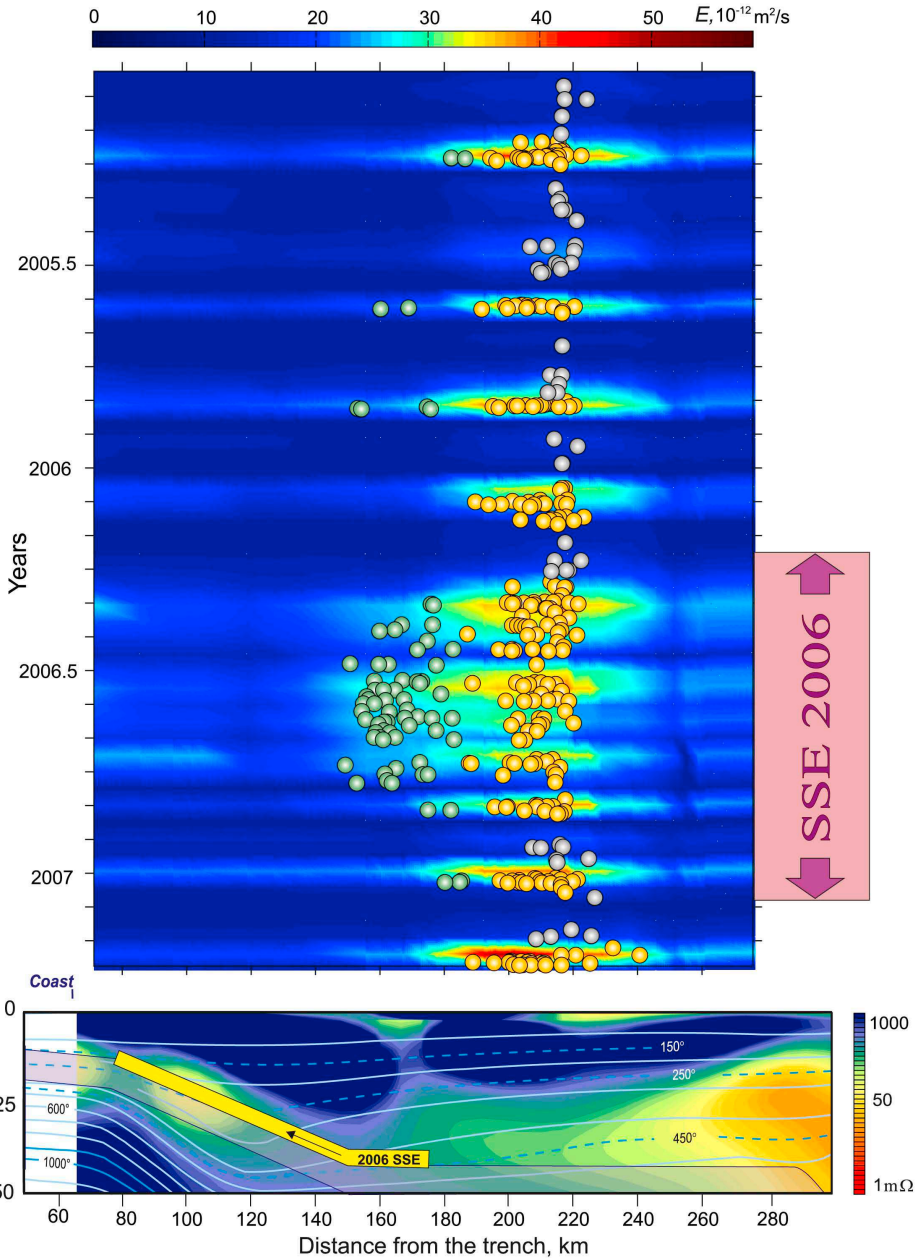
Figure 6. Normalized value of C from the inversion (Equation 1) related to the NVT duration, Δt, for the downdip high-energy NVT (orange dots) and the updip low-energy NVT (green dots). The gray dots are the inter-episode NVT's. These are the same events and color scheme shown in Figures 1 and 3. C is directly related to the seismic energy of the NVT at the source. **A** shows that C is roughly proportional to Δt as has been observed in other studies [*Aguiar et al.*, 2009], however the relation is very disperse. **B** shows the normalized value of $C/\Delta t$ over time.
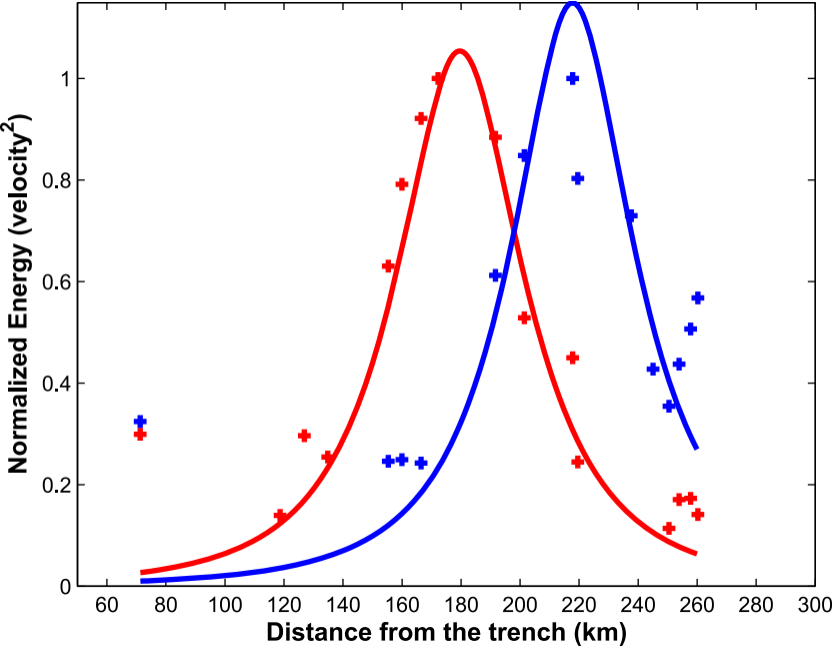
Figure 7. NVT epicenters from this article and the 2006 SSE slipping front from *Radiguet et al.* [2010]. The downdip, high-energy NVT (orange dots) and the updip, low-energy NVT (green dots) and the inter-episode NVT (gray dots) correspond to Figures 1, 3, 5, and 6. The sub-figures are in chronological order starting January 30, 2006 at the top and ending 350 days later January 15, 2007 at the bottom. Each sub-figure contains 50 days of NVT and slip.
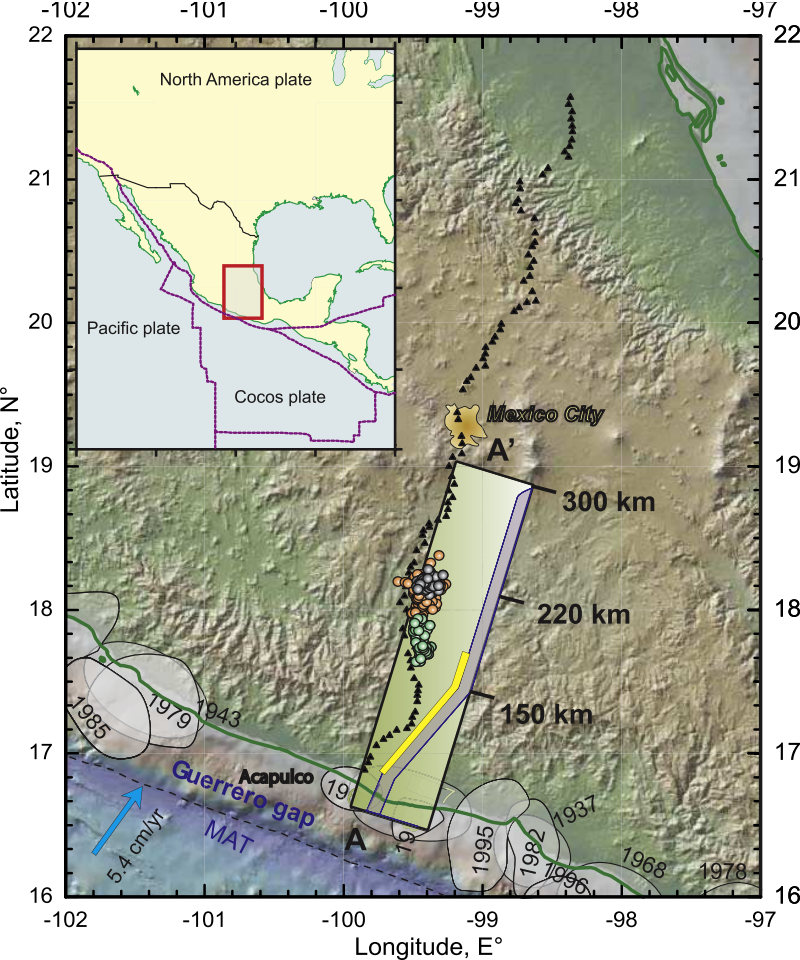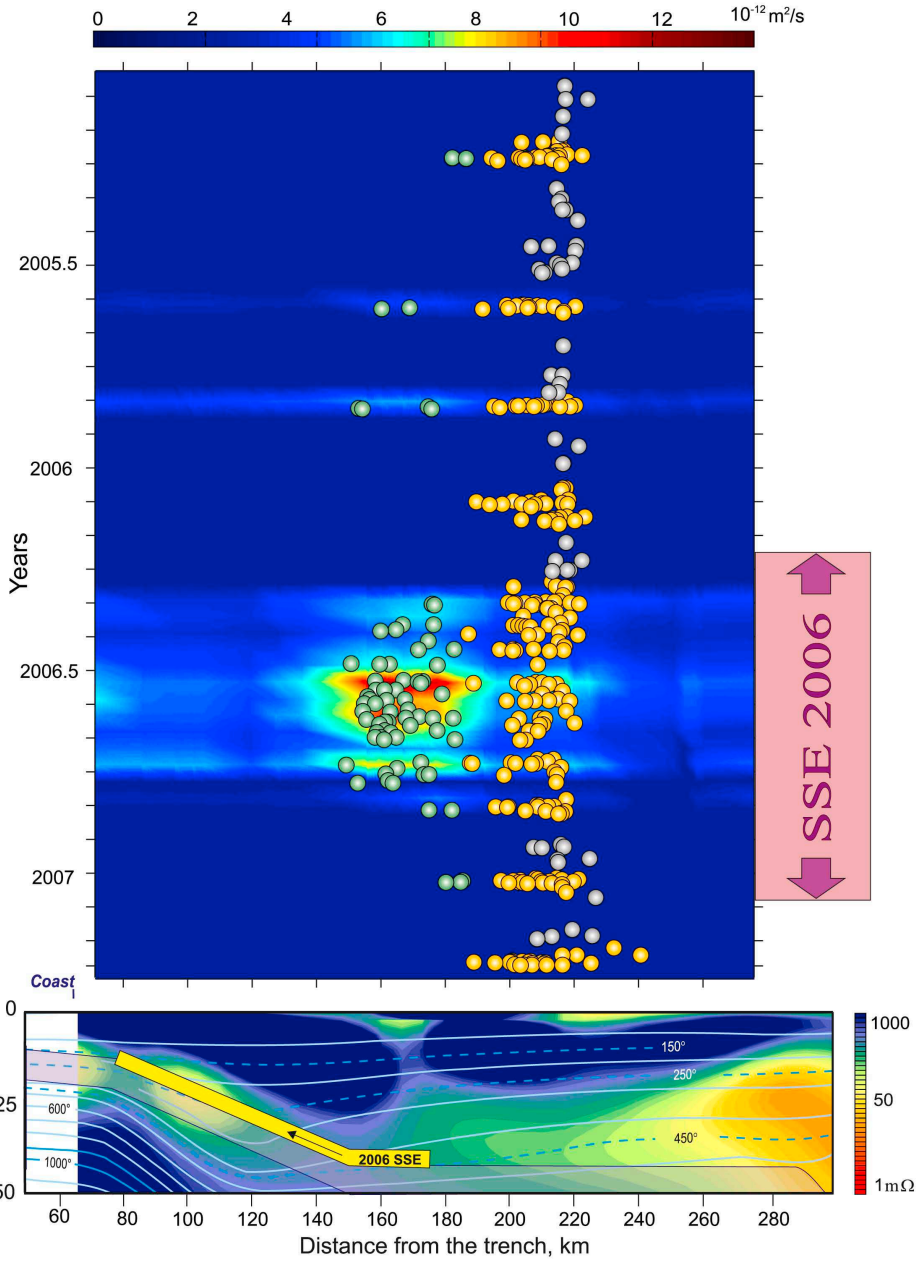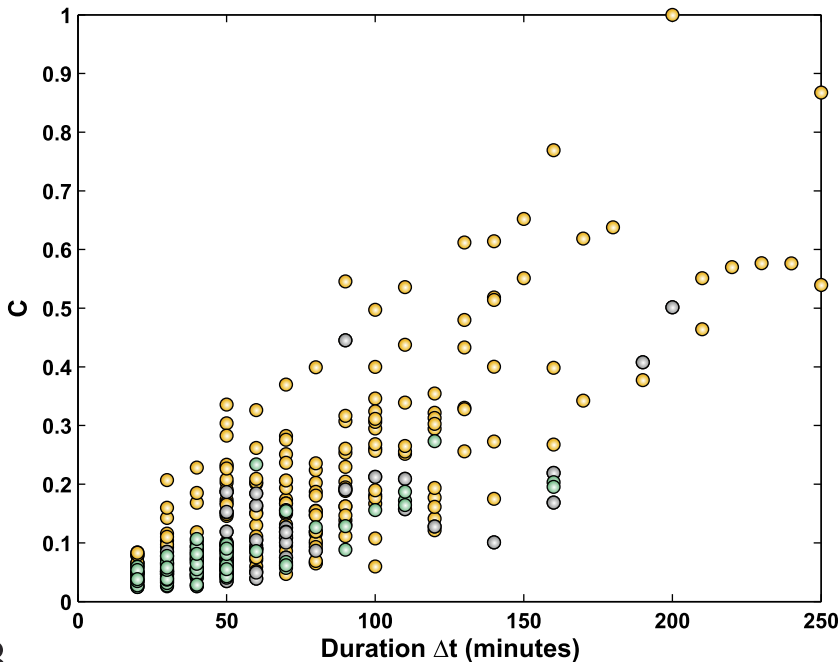
Example of tremor recorded March 21, 2005